Transactions of the Materials Research Society of Japan 29[6] 2773-2776 (2004)

High Temperature Thermoelectric Properties of the One-Dimensional $Ca_3Co_2O_6$ Compound

M. Mikami[1] and R. Funahashi[1,2]

1 CREST, Japan Science and Technology Agency, 1-8-31 Midorigaoka, Ikeda, Osaka 563-8577, Japan
Fax: 81-72-751-9622, e-mail: m-mikami@aist.go.jp

2 National Institute of Advanced Industrial Science and Technology, 1-8-31 Midorigaoka, Ikeda, Osaka 563-8577, Japan
Fax: 81-72-751-9622, e-mail: funahashi-r@ aist.go.jp

High-temperature thermoelectric properties of single-crystal $Ca_3Co_2O_6$, which consists of parallel one-dimensional $Co_2O_6^{6-}$ chains separated by Ca^{2+} ions, have been measured. The electrical resistivity (ρ) along the *c*-axis decreases rapidly with increasing temperature from 2×10^4 to 8 mΩcm in a temperature region of 300-1073 K. The Seebeck coefficient (S) is positive and is 160 μV/K at 1073 K. The thermal conductivity (κ) is as low as 8 W/mK at room temperature and decreases linearly with the increase of temperature to 4.6 W/mK at 773 K. Thus, the estimated dimensionless figure-of-merit, $ZT = (S^2/\rho\kappa)T$ (T: absolute temperature), is about 0.15 at 1073 K. As the thermoelectric figure-of-merit, Z, shows a sharp rise in the measured temperature range, $Ca_3Co_2O_6$ is expected to possess high thermoelectric efficiency at higher temperatures by virtue of being chemically stable up to 1300 K. In addition, in order to investigate the effect of partial substitution of transition metal for Co site, polycrystalline $Ca_3Co_2O_6$ and $Ca_3Co_{1.8}M_{0.2}O_6$ (M: Mn, Fe, Ni Cu) samples were prepared by solid-state reaction. We found that ρ can be reduced by Ni substitution without significant decrease in S. Thus, the power factor, $PF = (S^2/\rho)$, of $Ca_3Co_{1.8}Ni_{1.2}O_6$ is twice as large as non-substituted $Ca_3Co_2O_6$.

Key words: thermoelectrics, oxide, low-dimensional structure, single crystal

1. INTRODUCTION

Thermoelectric devices have recently attracted renewed interest in terms of their potential application to clean energy-conversion systems. The conversion efficiency of a thermoelectric material is evaluated by the figure-of-merit $Z = S^2/\rho\kappa$, where S is the Seebeck coefficient, ρ is the electrical resistivity and κ is the thermal conductivity. Oxides have thus been regarded as unsuitable for thermoelectric application because of their high ρ resulting from poor mobility. However, the recent discovery of large thermopower coexisting with low electrical resistivity in Na_xCoO_2 and $Ca_3Co_4O_9$ has opened the way to the exploration of oxide thermoelectric materials.[1-4] The single crystal of these cobalt oxides exhibits good thermoelectric performance, $ZT > 1$ at 1000 K,[2] competitive with conventional degenerate semiconductors such as Bi_2Te_3, PbTe and $Si_{1-x}Ge_x$. However, since these cobalt oxides decompose at around 1100 K, materials possessing greater stability at high temperatures are required for power generation from waste heat in higher temperature regions, such as 627-1773 K in the steel industry and 473-1223 K in the ceramic industry.

$Ca_3Co_2O_6$, which is a decomposed phase of $Ca_3Co_4O_9$, is chemically stable up to 1300 K.[5] This compound belongs to the A'_3ABO_6 formula oxides (A': Ca, Sr, Ba, A: Ni, Cu, Zn, B: Co, Ir, Pt).[6,7] As shown in Fig. 1, it consists of parallel one-dimensional $Co_2O_6^{6-}$ chains, which are built by successive alternating face-sharing CoO_6 trigonal prisms and CoO_6 octahedra along the hexagonal *c*-axis. Each chain is surrounded by six chains constituting a hexagonal arrangement. The chains are separated by octa-coordinated Ca^{2+} ions.[6] Though this compound is regarded as useless for thermoelectric applications because of its high electrical resistivity of 4 Ωcm at room temperature.[8,9] Its thermoelectric performance in high temperature regions has not been evaluated hitherto. In this study, the thermoelectric properties of $Ca_3Co_2O_6$ are examined in a temperature range of 300-1073 K using single-crystal specimens. Moreover, the effect of the partial substitution of transition metal for Co site is investigated using polycrystalline $Ca_3Co_2O_6$ and $Ca_3Co_{1.8}M_{0.2}O_6$ (M: Mn, Fe, Ni, Cu) samples.

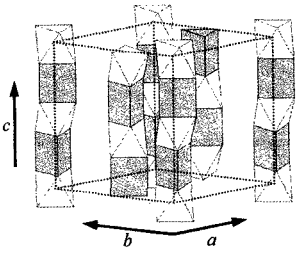

Fig. 1. Schematic illustrations of the crystal structure of $Ca_3Co_2O_6$. Open and shaded polyhedra represent CoO_6 octahedra and CoO_6 trigonal prisms, respectively. The $Co_2O_6^{6-}$ chain is surrounded by six chains constituting a hexagonal arrangement. The chains are separated by octa-coordinated Ca^{2+} ions.

2. EXPERIMENTAL

Single crystals of $Ca_3Co_2O_6$ were grown by a solution

method using a K_2CO_3-KCl flux. In the first step, polycrystalline $Ca_3Co_2O_6$ was prepared by solid-state reaction of a stoichiometric mixture of Co_3O_4 (99.9 %) and $CaCO_3$ (99.5 %). The mixture was sintered twice in air at 1223 K for 20 h. The prepared $Ca_3Co_2O_6$ powder and a mixture of K_2CO_3 and KCl in a molar ratio of 4:1 were mixed and loaded into an aluminum crucible having a 500 cm^3 volume. The powder was dissolved in the solution at 1173 K for 10 h. The solute concentration was 1.5 mol%. After this procedure, a platinum wire was inserted into the solution to induce nucleation, and the solution was subsequently cooled to 1073 K at a rate of 1 K/h. Two different kinds of crystals were grown on the platinum wire. These needle-shaped crystals and platelet-shaped crystals were identified as $Ca_3Co_2O_6$ and as $Ca_3Co_4O_9$, respectively, by structural and constituent analyses with powder X-ray diffraction (XRD) using Cu$K\alpha$ radiation and an energy dispersive X-ray (EDX) spectrometer. $Ca_3Co_2O_6$ single crystals of several mm length were mechanically isolated from the solidified material. The X-ray diffraction study of the crystals confirms that their length coincides with the c-axis of the hexagonal cell.

Polycrystalline $Ca_3Co_2O_6$ and $Ca_3Co_{1.8}M_{0.2}O_6$ (M: Mn, Fe, Ni, Cu) samples were synthesized by solid-state reaction. $CaCO_3$ (99.5 %), Co_3O_4 (99.9 %), Mn_2O_3 (99.9 %), Fe_2O_3 (99.9 %), NiO (99.9 %) and CuO (99.9 %) powders were used as starting materials. The stoichiometric mixtures of the starting materials were calcined at 1200 K for 20 h in air, pressed into pellets, then sintered at 1273 K for 20 h in air. Figure 2 shows the powder XRD patterns of the prepared polycrystalline samples. Almost all peaks are indexed as the reported $Ca_3Co_2O_6$ phase,[5] though tiny trace of NiO and Cu_2O is detected as marked with • in $Ca_3Co_{1.8}Ni_{0.2}O_6$ and $Ca_3Co_{1.8}Cu_{0.2}O_6$ sample, respectively. The pellets were cut into a rectangular-shaped specimen of 3 × 3 × 15 mm^3.

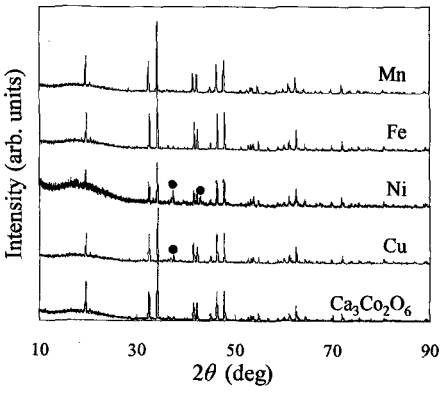

Fig. 2. Powder XRD patterns (Cu $K\alpha$ radiation) of the polycrystalline $Ca_3Co_2O_6$ and $Ca_3Co_{1.8}M_{0.2}O_6$ (M: Mn, Fe, Ni, Cu). Almost all peaks are assigned to $Ca_3Co_2O_6$ structure, though tiny trace of impurity phase of NiO and Cu_2O is detected as marked with • in $Ca_3Co_{1.8}Ni_{0.2}O_6$ and $Ca_3Co_{1.8}Cu_{0.2}O_6$ sample, respectively.

ρ of the single-crystal sample along the c-axis and the polycrystalline samples was measured at 300-1073 K in air using a conventional four-probe dc technique. S was calculated from a plot of thermoelectric voltage against temperature differential as measured at 373-1073 K in air using an instrument designed by our laboratory. Two Pt-Pt/Rh (R-type) thermocouples were attached to both ends of the samples using silver paste. The Pt wires of the thermocouples were used for voltage terminals. Measured S values were reduced by those of Pt wires to obtain the net S values of the samples. The thermal conductivity (κ) was evaluated from the density (D), the thermal diffusivity (α) and the heat capacity (C_p) given the relationship $\kappa = D \cdot \alpha \cdot C_p$.[10,11] D and C_p were measured by a pycnometer and by a differential scanning calorimeter, respectively. α was estimated by ac calorimetry associated with optical pulse heating.[12]

3. RESULTS AND DISCUSSION

3.1 Non-substituted $Ca_3Co_2O_6$ single-crystal

The temperature dependence of ρ of the single-crystal $Ca_3Co_2O_6$ along the Co_2O_6 chains (c-axis) is shown in Fig. 3. A thermally activated behavior is observed over the entire measured temperature range. The value of ρ decreases rapidly with increasing temperature. For instance, ρ of the single-crystal sample decreases from 2 × 10^4 to 8 mΩcm in a temperature range of 300-1073 K. As shown in an inset of Fig. 3, the relationship between log ρ and $T^{-1/2}$ is linear in the lower temperature region while a change of the inclination was observed at around 400 K. This can be attributed to the variable range hopping (VRH) conductivity,[13-16] $\rho=\rho_0\exp[(T_0/T)^{1/1+n}]$, assuming the dimensionality n to be 1. This one-dimensional transport character is consistent with the structure of $Ca_3Co_2O_6$, the metal-metal intrachain distance (2.595 Å) of which is short compared to the interchain separation (5.24 Å).[6] The T-dependence of VRH indicates the localized character of the carriers in the Co_2O_6 chains.

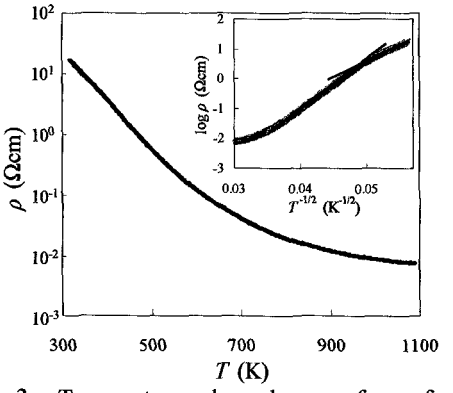

Fig. 3. Temperature dependence of ρ for the single-crystal $Ca_3Co_2O_6$ along the Co_2O_6 chains (c-axis). The inset shows log ρ as a function of $T^{-1/2}$.

S of the single-crystal $Ca_3Co_2O_6$ along the c-axis versus temperature is plotted in Fig. 4. The S-T curves also show a thermally activated behavior as seen in the T-dependence of ρ. The value of S is large and positive, indicating that the transport is dominated by p-type carriers. Though S decreases with increasing temperature, it remains as high as 160 μV/K at 1073 K in contrast to the significant reduction of ρ. By reduction of ρ in the higher temperature region, the value of power factors ($PF = S^2/\rho$) for the single-crystal $Ca_3Co_2O_6$ reaches 3.4 × 10^{-4} W/mK^2 at 1073 K.

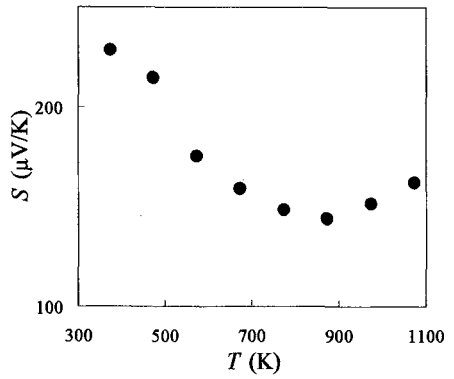

Fig. 4. Temperature dependence of S for the single-crystal $Ca_3Co_2O_6$ along the Co_2O_6 chains (c-axis).

Temperature dependence of κ for the $Ca_3Co_2O_6$ single-crystal is shown in Fig. 5. κ decreases linearly with increasing temperature. The dotted line in Fig. 5 expresses a linear extrapolation from κ measured in the measured temperature region of 300-773 K. From the extrapolation, the value of κ is 2.4 W/mK at 1073 K. In order to estimate the contributions from the electron term (κ_{ele}) and the phonon term (κ_{ph}) to the sum total κ, we apply the Wiedemann-Franz law ($\kappa_{ele} = L_0T/\rho$), where $L_0 = 2.44 \times 10^{-8}$ V^2/K^2 is the Lorentz number based on a free electron model. As shown in the inset of Fig. 5, κ is largely governed by κ_{ph}. The inverse relationship between the phonon thermal conductivity and T is given by the typical phonon mode.[17] However, the experimental result of κ_{ph} for $Ca_3Co_2O_6$ seems to have linear T-dependence. The one-dimensional structure of $Ca_3Co_2O_6$ may induce some kind of phonon scattering perpendicular to the one-dimensional $Co_2O_6^{6-}$ chains, though we cannot give a precise explanation at present.

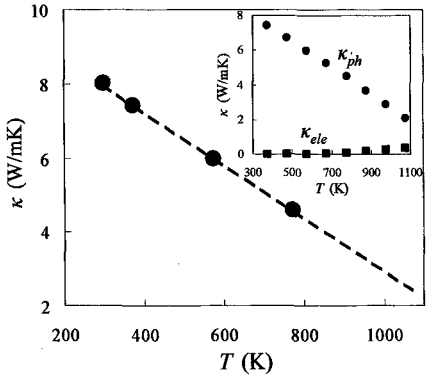

Fig. 5. Temperature dependence of κ for the single-crystal $Ca_3Co_2O_6$ along the c-axis. The inset shows electron term (κ_{ele}) and the phonon term (κ_{ph}) to the sum total κ as a function of T.

We calculated the thermoelectric figure-of-merit, $Z = S^2/\rho\kappa$, of the single-crystal $Ca_3Co_2O_6$. Values of extrapolated κ are used above 873 K. As shown in Fig. 6, the Z value increases with the increase of temperature, resulting from reduction of ρ and κ. The value of the dimensionless figure-of-merit, ZT, is about 0.15 at 1073 K. The $Ca_3Co_2O_6$ compound was confirmed to be chemically stable up to 1300 K by thermogravimetric analysis and differential thermal analysis (TG/DTA, Rigaku Co., Ltd., TG8120). Taking an optimistic view, Z may continuously increase at higher temperatures, such as 5×10^{-4} K^{-1} at 1300 K.

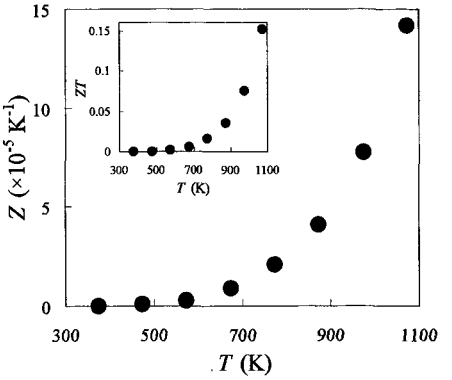

Fig. 6. Z for the single-crystal $Ca_3Co_2O_6$ along the c-axis vs T. The inset shows the ZT as a function of temperature.

3.2 Partial substitutions

The temperature dependence of ρ of the polycrystalline $Ca_3Co_2O_6$ and $Ca_3Co_{1.8}M_{0.2}O_6$ (M: Mn, Fe, Ni, Cu) samples is shown in Fig. 7. A thermally activated behavior is observed in every ρ-T curves in different activation energies. The increase in the value of ρ occurs in all the partially substituted samples except Ni-substituted one at high temperatures. ρ of the $Ca_3Co_{1.8}Ni_{0.2}O_6$ sample is 30 mΩcm, which is twice as low as that of the non-substituted $Ca_3Co_2O_6$, at 1000 K.

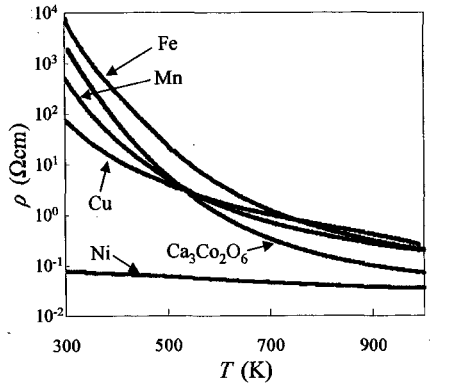

Fig. 7. Temperature dependence of ρ for the polycrystalline $Ca_3Co_2O_6$ and $Ca_3Co_{1.8}M_{0.2}O_6$ (M: Mn, Fe, Ni, Cu) samples.

S of the polycrystalline $Ca_3Co_2O_6$ and $Ca_3Co_{1.8}M_{0.2}O_6$ (M: Mn, Fe, Ni, Cu) samples versus temperature is plotted in Fig. 8. The values of S are large and positive, indicating that the transport is dominated by p-type carriers. Partially substituted samples except $Ca_3Co_{1.8}Fe_{0.2}O_6$ is different from non-substituted sample in T-dependence of S. Especially in Ni-substituted one, S shows metallic T-dependence, increase with increasing temperature. Considering that ρ of the $Ca_3Co_{1.8}Ni_{0.2}O_6$ is twenty thousand times lower than that of the $Ca_3Co_2O_6$ at room temperature, carriers may be significantly doped by partial Ni-substitution. As shown in Fig. 9, PF of the

polycrystalline $Ca_3Co_{1.8}Ni_{0.2}O_6$ sample is 100-2 times larger than that of the non-substituted $Ca_3Co_2O_6$ one at temperature region of 373-973 K, resulting from reduction of ρ without significant decrease in S. Thus, it is expected that the substitution of Ni for Co site improve the thermoelectric efficiency of $Ca_3Co_2O_6$ compound.

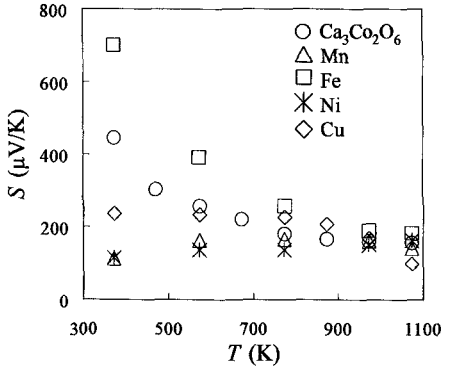

Fig. 8. S for the polycrystalline $Ca_3Co_2O_6$ and $Ca_3Co_{1.8}M_{0.2}O_6$ (M: Mn, Fe, Ni, Cu) samples vs T.

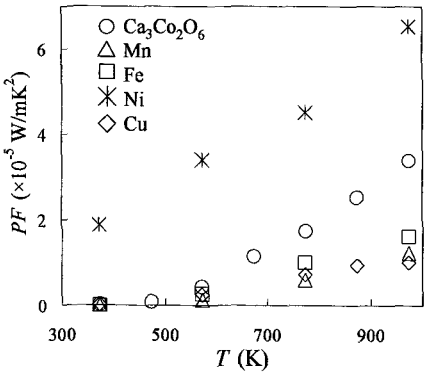

Fig. 9. PF of the polycrystalline $Ca_3Co_2O_6$ and $Ca_3Co_{1.8}M_{0.2}O_6$ (M: Mn, Fe, Ni, Cu) samples as a function of temperature.

4. CONCLUSION

We evaluated the high-temperature thermoelectric properties of single-crystal $Ca_3Co_2O_6$ and polycrystalline $Ca_3Co_2O_6$ and $Ca_3Co_{1.8}M_{0.2}O_6$ (M: Mn, Fe, Ni, Cu) samples. ρ and S of the single-crystal $Ca_3Co_2O_6$ along the c-axis are 8 mΩcm and 160 μV/K, respectively, at 1073 K. κ decreases linearly to 4.6 W/mK with the increasing temperature to 773 K. The linearly extrapolated value of κ is 2.4 W/mK at 1073 K. Accordingly, the estimated ZT is about 0.15 at 1073 K. As Z shows a sharp rise with increasing temperature in the measured temperature range, $Ca_3Co_2O_6$ is expected to possess high thermoelectric efficiency at higher temperatures. Since it was confirmed that the $Ca_3Co_2O_6$ is chemically stable up to 1300 K, the title compound is considered a potential candidate for use as a thermoelectric material at high temperatures, such as thermoelectric power generation in advanced radioisotope and nuclear reactor power systems for planetary exploration. Moreover, PF of the polycrystalline $Ca_3Co_{1.8}Ni_{0.2}O_6$ sample is twice as large as that of the non-substituted $Ca_3Co_2O_6$ one at 973 K, resulting from reduction of ρ without significant decrease of S. Therefore, it is expected that the substitution of Ni for Co site improve the thermoelectric efficiency of $Ca_3Co_2O_6$ compound. In further investigation, the effects of the Ni-substitution will be precisely examined using single crystal specimens.

Acknowledgment

The authors would like to thank T. Inoue and S. Sodeoka for technical support in thermal conductivity measurement.

References

[1] I.Terasaki, Y. Sasago and K. Uchinokura, Phys. Rev. B 56, 12685 (1997).
[2] K. Fujita, T. Mochida and K. Nakamura, Jpn. J. Appl. Phys. 40, 4644 (2001).
[3] S. Li, R. Funahashi, I. Matsubara, K. Ueno and H. Yamada, J. Mater. Chem. 9, 1659 (1999).
[4] R. Funahashi, I. Matsubara, H. Ikuta, T. Takeuchi, U. Mizutani and S. Sodeoka, Jpn. J. Appl. Phys. 39, L1127 (2000).
[5] E. Woermann and A. Muan, J. Inorg. Nucl. Chem. 32, 1457 (1970).
[6] H. Fjellvåg, E. Gulbrandsen, S. Aasland. A. Olsen and B. C. Hauback, J. Solid State Chem 124, 190 (1996).
[7] K. Boulahya, M. Parras and J. M. González-Calbet, J. Solid State Chem 145, 166 (1999).
[8] A. Maignan, C. Michel, A. C. Masset, C. Mertin and B. Raveau, Eur. Phys. J. B 15, 657 (2000).
[9] B. Raquet, M. N. Baibich, J. M. Broto, H. Rakoto, S. Lambert and A. Maignan, Phys. Rev. B 65, 104442 (2002).
[10] I. Hatta, Y. Sasuga, K. Kato and A. Maesono, Rev. Sci. Instrum. 56, 1643 (1985).
[11] T. Yamane, S. Katayama and M. Todoki, Rev. Sci. Instrum. 66, 5305 (1995).
[12] Long-Jye Sheu and Jenn-Der Lin, Jpn. J. Appl. Phys. 39, L690 (2000).
[13] N. F. Mott, J. Non-Cryst. Solid. 1, 1 (1968).
[14] N. F. Mott and E. A. Davis, "Electronic Processes in Non-crystalline Materials", Oxford, Claredon (1979).
[15] A. L. Efros and B. I. Shklovskii, J. Phys. C 8, L49 (1975).
[16] B. I. Shklovskii and A. L. Efros, "Electronic Properties of Doped Semiconductors", Springer, Berlin (1984).
[17] J. M. Ziman, "Principles of the Theory of Solids", 2nd ed., Cambridge University Press, Cambridge (1972).

(Received October 13, 2003; Accepted January 16, 2004)